

# Cosmological parameters from complementary observations of the Universe

R. Durrer<sup>1★</sup> and B. Novosyadlyj<sup>2</sup>

<sup>1</sup>*Department de Physique Théorique, Université de Genève, Quai Ernest Ansermet 24, CH-1211 Genève 4, Switzerland*

<sup>2</sup>*Astronomical Observatory of National University of L'viv, Kyryla and Mephodia str. 8, 290005 L'viv, Ukraine*

Accepted 2000 December 14. Received 2000 December 7; in original form 2000 September 6

## ABSTRACT

We use observational data on the large-scale structure (LSS) of the Universe measured over a wide range of scales, from subgalactic up to horizon scale, and on the cosmic microwave background anisotropies to determine cosmological parameters within the class of adiabatic inflationary models. We show that a mixed dark matter model with cosmological constant ( $\Lambda$ MDM model) and parameters  $\Omega_m = 0.37^{+0.25}_{-0.15}$ ,  $\Omega_\Lambda = 0.69^{+0.15}_{-0.20}$ ,  $\Omega_\nu = 0.03^{+0.07}_{-0.03}$ ,  $N_\nu = 1$ ,  $\Omega_b = 0.037^{+0.033}_{-0.018}$ ,  $n_s = 1.02^{+0.09}_{-0.10}$ ,  $h = 0.71^{+0.22}_{-0.19}$ ,  $b_{cl} = 2.4^{+0.7}_{-0.7}$  ( $1\sigma$  confidence limits) matches observational data on LSS, the nucleosynthesis constraint, direct measurements of the Hubble constant, the high-redshift supernova type Ia results and the recent measurements of the location and amplitude of the first acoustic peak in the cosmic microwave background (CMB) anisotropy power spectrum. The best model is  $\Lambda$ -dominated (65 per cent of the total energy density) and has slightly positive curvature,  $\Omega = 1.06$ . The clustered matter consists of 8 per cent massive neutrinos, 10 per cent baryons and 82 per cent cold dark matter (CDM). The upper  $2\sigma$  limit on the neutrino content can be expressed in the form  $\Omega_\nu h^2 / N_\nu^{0.64} \leq 0.042$  or, via the neutrino mass,  $m_\nu \leq 4.0$  eV. The upper  $1(2)\sigma$  limit for the contribution of a tensor mode to the *COBE* DMR data is  $T/S < 1(1.5)$ . Furthermore, it is shown that the LSS observations, together with the Boomerang (+MAXIMA-1) data on the first acoustic peak, rule out zero- $\Lambda$  models at more than a  $2\sigma$  confidence limit.

**Key words:** cosmic microwave background – cosmological parameters – cosmology: theory – dark matter – large-scale structure of Universe.

## 1 INTRODUCTION

In the last decade of this century we have obtained important experimental results which play a crucial role for cosmology: the *Cosmic Background Explorer (COBE)* has discovered the large-scale anisotropies of the cosmic microwave background radiation (Bennett et al. 1996); the High-Z Supernova Collaboration (Riess et al. 1998) and the Supernova Cosmology Project (Perlmutter et al. 1998) found that the Universe is accelerating rather than decelerating; the Super-Kamiokande experiment (Fukuda et al. 1998) discovered neutrino oscillations that prove the existence of neutrinos with non-zero rest mass; balloon-borne measurements of the cosmic microwave background (CMB) temperature fluctuations by Boomerang (de Bernardis et al. 2000) and MAXIMA-1 (Hanany et al. 2000) have measured the height, position and width of the first acoustic peak, which is in superb agreement with an adiabatic scenario of galaxy formation.

On the other hand, the comparison of recent experimental data

on the large-scale structure of the Universe with theoretical predictions of inflationary cosmology have shown for quite some time that the simplest cold dark matter (CDM) model is ruled out and we have to allow for a wider set of parameters to fit all observational data on the status and history of our Universe. These include spatial curvature ( $\Omega_k$ ), a cosmological constant ( $\Omega_\Lambda$ ), the Hubble parameter [ $h \equiv H_0 / (100 \text{ km s}^{-1} \text{ Mpc}^{-1})$ ], the energy density of baryonic matter ( $\Omega_b$ ), cold dark matter ( $\Omega_{\text{cdm}}$ ), the number of species of massive neutrinos ( $N_\nu$ ) and their density ( $\Omega_\nu$ ), the amplitude of the power spectra of primordial perturbations in scalar ( $A_s$ ) and tensor ( $A_t$ ) modes and the corresponding power-law indices ( $n_s$  and  $n_t$ ), and the optical depth to early reionization ( $\tau$ ). Constraining this multidimensional parameter space determining the true values of fundamental cosmological parameters, the nature and content of the matter which fills our Universe is an important and exciting problem of cosmology which has now become feasible because of the enormous progress in cosmological observations. About a dozen or more papers have been devoted to this problem in the last couple of years (see e.g. Lineweaver 1998; Lineweaver & Barbosa 1998; Bridle et al. 1999;

★ E-mail: ruth.durrer@physics.unige.ch

Efstathiou & Bond 1999; Tegmark 1999; Balbi et al. 2000; Hu et al. 2001; Lange et al. 2001; Lyth & Covi 2000; Merchiorri et al. 2000; Novosyadlyj et al. 2000a,b; Tegmark & Zaldarriaga 2000a,b; Tegmark, Zaldarriaga & Hamilton 2001; some reviews are found in Durrer & Straumann 1999; Primack 2000; Primack & Gross 2000; Sahni & Starobinsky 2000 and references therein).

However, in spite of these intensive investigations the problem is still not satisfactorily resolved. Some of the remaining issues are explained below.

First of all, we would like to have observations that ‘measure’ cosmological parameters in as model-independent a way as possible. Clearly, most values of cosmological parameters obtained from observations of large-scale structure, galaxy clustering and CMB anisotropies are strongly model-dependent. If the ‘correct’ model of structure formation is not within the family investigated, we may not notice it, especially if the error bars are relatively large. This leads us to the next problem. Even if cosmological observations have improved drastically, we still need more accurate data with better defined statistical properties (e.g. we need to know the correlation of different measurements). The new CMB anisotropy data are already of this quality but the galaxy and cluster data are still relatively far from it.

A next important point is the correspondence between theoretical predictions and observational characteristics used in the analysis. We have to find a fast but accurate way to compute the theoretical values, especially when exploring high-dimensional parameter spaces. All parameters must be fitted simultaneously, which renders the problem computationally complicated and very time-consuming. Owing to this difficulty, many authors search some subset of parameters, setting the others to some fixed ‘reasonable’ priors, thereby investigating a subclass of cosmological models. As different authors also use different subsets of observational data, the resulting cosmological parameters still vary in a relatively wide range.

Another problem is the degeneracies in that appear in parameter space, especially in the case when only CMB anisotropy data are used (Efstathiou & Bond 1999). It can be reduced substantially or even removed completely if galaxy clustering data, corresponding to different scales and redshifts, are combined with CMB measurements. This idea has already been employed on several occasions and is known under the name ‘cosmic concordance’ (for a recent review see Tegmark et al. 2000).

The goal of this paper is to determine cosmological parameters of the subclass of models without a tensor mode and no early reionization on the basis of LSS data related to different scales and different redshifts. In Novosyadlyj et al. (2000a) we have used the same approach to test flat models; we have shown that  $\Lambda$ MDM models are preferred in this class of models. There we have also shown that pure CDM models with  $h \geq 0.5$ , scale-invariant primordial power spectrum, vanishing cosmological constant and spatial curvature are ruled out at very high confidence level, more than 99.99 per cent. The corresponding class of mixed dark matter (MDM) models are ruled out at about 95 per cent confidence level. It was noted (Novosyadlyj et al. 2000b) that the galaxy clustering data set determines the amplitude of scalar fluctuations approximately at the same level as the *COBE* four-year data. This indicates that a possible tensor component in the *COBE* data cannot be very substantial.

In this paper we test  $\Lambda$ MDM models with non-zero curvature. Furthermore, we use the data on the location and amplitude of the first acoustic peak determined from the most accurate recent measurements of the CMB power spectrum. The data on the

amplitude of the second and third peaks are used as an additional test for the model preferred by large-scale structure, *COBE* and first peak data. We investigate the (in-)consistency of our data set with the second and third peaks. We also use the SNIa constraint for comparison.

The outline of the paper is as follows. In Section 2 we describe the experimental data set that is used here. The calculations of theoretical predictions and the method employed to determine cosmological parameters are described in Section 3. In Section 4 we discuss our results and compare them with other investigations. Our conclusions are presented in Section 5.

## 2 THE EXPERIMENTAL DATA SET

Our approach is based on the quantitative comparison of the theoretical predictions for the characteristics of the large-scale structure of the Universe with corresponding observational ones. Theoretical predictions are calculated on the basis of an initial power spectrum of density perturbations, the shape of which strongly depends on all parameters supposed here for determination. Model-independent observational constraints on the inclination and amplitude of the power spectrum at different scales will therefore be used in this search.

### 2.1 CMB data

We use the *COBE* 4-yr data on CMB temperature anisotropies (Bennett et al. 1996) to normalize the density fluctuation power spectra according to Liddle et al. (1996) and Bunn & White (1997). Therefore, each model will match the *COBE* data by construction.

We believe that using all available experimental data on  $\Delta T/T$  at angular scales smaller than the *COBE* measurement is not an optimal way to search best-fitting cosmological parameters, owing to their large dispersion (see for examples fig. 10.1 of Durrer & Straumann 1999, fig. 2 of Novosyadlyj et al. 2000a or fig. 1 of Tegmark et al. 2000), which together with the large number of experimental points,  $\sim 70$  stipulating a high degrees of freedom, results in wide ranges for the confidence limits on cosmological parameters. The Boomerang (de Bernardis et al. 2000) and MAXIMA-1 (Hanany et al. 2000) experiments represent a new generation of CMB measurements. They have produced a CMB map of about  $\sim 100 \text{ deg}^2$  with a resolution better than half a degree and a  $S/N \sim 2$ , which allows us to determine the location and amplitude of the first acoustic peak with high accuracy. The position of the first and amplitudes of the first, second and third acoustic peaks in the angular power spectrum of the CMB temperature fluctuations together with the *COBE* data are the main measured characteristics of the CMB power spectrum. They contain information about amplitude and tilt of the primordial power spectrum of density fluctuations at largest scales, from a few tens of Mpc up to the current horizon scale of several thousand Mpc. They are mainly sensitive to the parameters  $\Omega_k$ ,  $\Omega_m h^2$ ,  $\Omega_\Lambda$ ,  $\Omega_b h^2$  and  $n_s$  and to the normalization of the initial power spectrum of density fluctuations.

For example, the Boomerang data indicate that the first peak is located at the Legendre multipole  $\tilde{\ell}_p = 197 \pm 6$  and has an amplitude of  $\tilde{A}_p = 69 \pm 8 \mu\text{K}$  (this  $1\sigma$  error includes statistical and calibration errors). Here and in the following, a tilde denotes observed quantities. We use these results in our search procedure. The MAXIMA-1 data ( $\tilde{\ell}_p \approx 220$ ,  $\tilde{A}_p = 78 \pm 6 \mu\text{K}$ ) marginally

match Boomerang data and we will show that using them in combination with Boomerang data does not change the results significantly. The positions of the second and third peaks are not well determined, and we will not use them in the main search procedure but we use their amplitudes as determined by (Hu et al. 2001) for comparison with the predictions of our best-fitting model.

## 2.2 Rich cluster data

The important constraints on the form and amplitude of the matter power spectrum in the range from  $10h^{-1}\text{Mpc}$  up to scales approaching  $1000h^{-1}\text{Mpc}$  can be obtained from the study of clusters of galaxies, their space distribution, mass and X-ray temperature functions.

The power spectrum reconstructed from the observed space distribution of clusters has been determined many times for different samples from Abell, ACO and APM catalogues (see Einasto et al. 1997; Retzlaff et al. 1998; Tadros, Efstathiou & Dalton 1998; Miller & Batuski 2000 and references therein). The remarkable feature of the determinations by different groups is similar slopes of cluster power spectra on scales  $0.02h\text{Mpc}^{-1} \leq k \leq 0.1h\text{Mpc}^{-1}$ ,  $n \sim -1.5$  (see above-mentioned references). Here, we use the power spectrum of Abell-ACO clusters  $\bar{P}_{\text{A+ACO}}(k_j)$  (Retzlaff et al. 1998) as observational input. It is measured in the range  $0.03h\text{Mpc}^{-1} \leq k \leq 0.2h\text{Mpc}^{-1}$ , where effects of non-linear evolution are negligible, and it has well-analysed sources of uncertainties. The cluster power spectrum is biased with respect to the dark matter distribution. We assume that the bias is linear and scale-independent. This is reasonable in the range of scales considered as predicted from local bias models (Fry & Gaztañaga 1993) and indicated by numerical simulations (Benson et al. 2000). In our previous paper (Novosyadlyj et al. 2000a) we have shown that not all the 13 points given in Retzlaff et al. (1998) are independent measurements and the effective number of degrees of freedom is 3. However, to make best use of the observational information we use all 13 points of the power spectrum to determine cosmological parameters and assign  $n_F = 3$  for the number of degrees of freedom in the marginalization procedure.

A constraint for the amplitude of the fluctuation power spectrum on cluster scales can be derived from the cluster mass and the X-ray temperature functions. It is usually formulated as a constraint for the density fluctuation in a top-hat sphere of  $8h^{-1}\text{Mpc}$  radius,  $\sigma_8$ , which can be calculated for a given initial power spectrum  $P(k)$  by

$$\sigma_8^2 = \frac{1}{2\pi^2} \int_0^\infty k^2 P(k) W^2(8\text{Mpc } k/h) dk, \quad (1)$$

where  $W(x) = 3(\sin x - x \cos x)/x^3$  is the Fourier transform of a top-hat window function. Recent optical determinations of the mass function of nearby galaxy clusters (Girardi et al. 1998) give

$$\tilde{\sigma}_8 \Omega_m^{\alpha_1} = 0.60 \pm 0.04, \quad (2)$$

where  $\alpha_1 = 0.46 - 0.09\Omega_m$  for flat low-density models and  $\alpha_1 = 0.48 - 0.17\Omega_m$  for open models (at the 90 per cent confidence level). Several groups have found similar results using different methods and different data sets (for a comprehensive list of references see Borgani et al. 1999). This constraint on  $\sigma_8$  is exponentially sensitive and thus allows only very small error bars. If the theory is correct, this is of course a great advantage.

However, if our understanding of cluster formation is not entirely correct, this will lead to discrepancies with other experimental constraints.

From the observed evolution of the cluster X-ray temperature distribution function between  $z = 0.05$  and  $z = 0.32$  we use the following constraint derived by Viana & Liddle (1999):

$$\tilde{\sigma}_8 \Omega_m^{\alpha_2} = 0.56 \pm 0.19 \Omega_m^{0.1 \lg \Omega_m + \alpha_2}, \quad \alpha_2 = 0.34$$

for open models and

$$\tilde{\sigma}_8 \Omega_m^{\alpha_2} = 0.56 \pm 0.19 \Omega_m^{0.2 \lg \Omega_m + \alpha_2}, \quad \alpha_2 = 0.47$$

for flat models (both with 95 per cent confidence limits).

From the existence of three very massive clusters of galaxies observed so far at  $z > 0.5$  an additional constraint has been established by Bahcall & Fan 1998:

$$\tilde{\sigma}_8 \Omega_m^{\alpha_3} = 0.8 \pm 0.1, \quad (3)$$

where  $\alpha_3 = 0.24$  for open models and  $\alpha_3 = 0.29$  for flat models.

Note that all these constraints are given by slightly different formulae for either  $\Omega_\Lambda = 0$  or  $\Omega_\Lambda + \Omega_m = 1$ . However, we are going to use them for arbitrary values of  $\Omega_\Lambda$  and  $\Omega_m$ . As our best-fitting models are relatively close to the flat model, we mainly use the formula for the flat case. We have checked that our results are insensitive to this choice.

## 2.3 Peculiar velocity data

As our approach is based on the initial power spectrum of density fluctuations, it seems most favourable to use the power spectrum reconstructed from the observed space distribution of galaxies. However, the galaxy power spectra obtained from the two-dimensional APM survey (e.g. Maddox, Efstathiou & Sutherland 1996; Tadros & Sutherland 1996, and references therein), the CfA redshift survey (Vogeley et al. 1992; Park et al. 1994), the IRAS survey (Saunders et al. 1992; Saunders et al. 2000) and the Las Campanas Redshift Survey (da Costa et al. 1994; Landy et al. 1996) differ significantly in both the amplitude and the position of the maximum. Moreover, non-linear effects on small scales must be taken into account in their analysis. On the other hand, these power spectra contain large number of experimental points which are not independent and a decorrelation procedure for these power spectra must be employed. For these reasons and also in order to test the consistency between different data sets, we do not include galaxy power spectra for the determination of parameters in this work. It will be interesting to compare our best-fitting parameters with those obtained in analyses including galaxy power spectra.

Another constraint on the amplitude of the linear power spectrum of density fluctuations in our vicinity comes from the study of bulk flows of galaxies in spheres of large enough radii around our position. As these data may be influenced by the local supercluster (cosmic variance), we will use only the value of the bulk motion – the mean peculiar velocity of galaxies in a sphere of radius  $50h^{-1}\text{Mpc}$  given by Kolatt & Dekel 1997,

$$\tilde{V}_{50} = (375 \pm 85) \text{ km s}^{-1}. \quad (4)$$

With its generous error bars, this value is in a good agreement with other measurements of bulk motion at the scale  $40\text{--}60h^{-1}\text{Mpc}$  (Bertschinger et al. 1990; Courteau et al. 1993; Dekel 1994; see also the review by Dekel 1999).

## 2.4 Ly $\alpha$ constraints

An important constraint on the linear matter power spectrum on small scales [ $k \sim (2-4) h \text{Mpc}^{-1}$ ] comes from the Ly $\alpha$  forest, the Ly $\alpha$  absorption lines seen in quasar spectra (see Gnedin 1998, Croft et al. 1998 and references therein). Assuming that the Ly $\alpha$  forest is formed by discrete clouds with a physical size close to the Jeans scale in the reionized intergalactic medium at  $z \sim 2-4$ , Gnedin (1998) has derived a constraint on the value of the rms linear density fluctuations,

$$1.6 < \tilde{\sigma}_F(z=3) < 2.6 \quad (95 \text{ per cent confidence level})$$

$$\text{at } k_F \approx 34\Omega_m^{1/2} h \text{Mpc}^{-1}. \quad (5)$$

Taking into account the new data on quasar absorption lines, the effective equation of state and the temperature of the intergalactic medium at high redshift were re-estimated recently (Ricotti, Gnedin & Shull 2000). As a result the value of Jeans scale at  $z = 3$  has moved to  $k_F \approx 38\Omega_m^{1/2} h \text{Mpc}^{-1}$  (Gnedin, private communication). Here, we adopt this new value.

The procedure to recover the linear power spectrum from the Ly $\alpha$  forest has been elaborated by Croft et al. (1998). Analysing the absorption lines in a sample of 19 QSO spectra, they have obtained the following constraint on the amplitude and slope of the linear power spectrum at  $z = 2.5$  and  $k_p = 1.5\Omega_m^{1/2} h \text{Mpc}^{-1}$ ,

$$\tilde{\Delta}_p^2(k_p) \equiv k_p^3 P(k_p) / 2\pi^2 = 0.57 \pm 0.26, \quad (6)$$

$$\tilde{n}_p \equiv \frac{\Delta \log P(k)}{\Delta \log k} \Big|_{k_p} = -2.25 \pm 0.18, \quad (7)$$

at ( $1\sigma$  confidence level). The like constraints on the amplitude and slope of the linear power spectrum were obtained by (McDonald et al. 2000) from the analysis of absorption lines in a sample of eight QSOs. We will analyse these constraints in the context of our task and compare them with previous two. In the main search procedure, however, we will use the constraints given by Croft et al. (1998) as based on the more extensive sample of quasars.

## 2.5 Other experimental constraints

In addition to the CMB and LSS measurements described above, we also use some results of global observations which are independent of the LSS model. For the value of the Hubble constant we set

$$\tilde{h} = 0.65 \pm 0.10, \quad (8)$$

which is a compromise between measurements made by two groups, Tammann & Federspiel (1997) and Madore et al. (1999). We also employ a nucleosynthesis constraint on the baryon density deduced from the determination of the primeval deuterium abundance,

$$\tilde{\Omega}_b h^2 = 0.019 \pm 0.0024 \quad (95 \text{ per cent confidence level}), \quad (9)$$

given by Burles et al. (1999). The new, more precise determination (Burles, Nollett & Turner 2001) confirms this value.

Furthermore, we include the distance measurements of supernovae of type Ia (SNIa), which constrain the cosmic expansion history (Riess et al. 1998; Perlmutter et al. 1998, 1999). In a universe with cosmological constant this gives an important constraint on a combination of the values of the curvature, the cosmological constant and the matter content of the Universe. We

use the following constraint in our parameter search (Perlmutter et al. 1999):

$$[\Omega_m - 0.75\Omega_\Lambda] = -0.25 \pm 0.125. \quad (10)$$

## 3 THE METHOD AND SOME TESTS

One of the main ingredients for the solution to our search problem is a reasonably fast and accurate determination of the linear transfer function for dark matter clustering, which depends on the cosmological parameters. We use accurate analytical approximations of the MDM transfer function  $T(k; z)$  depending on the parameters  $\Omega_m$ ,  $\Omega_b$ ,  $\Omega_\nu$ ,  $N_\nu$  and  $h$  by Eisenstein & Hu (1999). According to this work, the linear power spectrum of matter density fluctuations is given by

$$P(k; z) = A_s k^{n_s} T^2(k; z) D_1^2(z) / D_1^2(0), \quad (11)$$

where  $A_s$  is the normalization constant for scalar perturbations and  $D_1(z)$  is the linear growth factor, which can be approximated by (Carroll, Press & Turner 1992)

$$D_1(z) = \frac{5}{2} \frac{\Omega_m(z)}{1+z} \left[ \frac{1}{70} + \frac{209\Omega_m(z) - \Omega_m^2(z)}{140} + \Omega_m^{4/7}(z) \right]^{-1},$$

where

$$\Omega_m(z) = \Omega_m(1+z)^3 / [\Omega_m(1+z)^3 + \Omega_\Lambda + \Omega_k(1+z)^2].$$

We normalize the spectra to the 4-year *COBE* data, which determine the amplitude of the density perturbation at the horizon scale,  $\delta_h$  (Liddle et al. 1996; Bunn & White 1997). The normalization constant  $A_s$  is then given by

$$A_s = 2\pi^2 \delta_h^2 (3000 \text{Mpc } h^{-1})^{3+n_s}. \quad (12)$$

The Abell-ACO power spectrum is related to the matter power spectrum at  $z = 0$ ,  $P(k; 0)$  by the cluster biasing parameter  $b_{cl}$ . As argued above, we assume scale-independent, linear bias

$$P_{A+ACO}(k) = b_{cl}^2 P(k; 0). \quad (13)$$

For a given set of parameters  $\Omega_m$ ,  $\Omega_\Lambda$ ,  $\Omega_b$ ,  $\Omega_\nu$ ,  $N_\nu$ ,  $n_s$ ,  $h$ , and  $b_{cl}$  the theoretical values of  $P_{A+ACO}(k_j)$  can now be obtained for the values  $k_j$  (table 1 of Novosyadlyj et al. 2000a). We denote them by  $y_j$  ( $j = 1, \dots, 13$ ).

The dependence of the position and amplitude of the first acoustic peak in the CMB power spectrum on cosmological parameters has been investigated using CMBFAST (Seljak & Zaldarriaga 1996). As expected, and as we have shown in our previous paper (Novosyadlyj et al. 2000a), the results are, within reasonable accuracy, independent of the fraction of hot dark matter,  $f_\nu = \Omega_\nu / \Omega_m$ , up to  $f_\nu \sim 0.6$ .

For the remaining parameters,  $n_s$ ,  $h$ ,  $\Omega_b$ ,  $\Omega_{cdm}$  and  $\Omega_\Lambda$ , we determine the resulting values  $\ell_p$  and  $A_p$  using the analytical approximation given by Efstathiou & Bond (1999). We extend the approximation to models with non-zero curvature ( $\Omega_k \equiv 1 - \Omega_m - \Omega_\Lambda \neq 0$ ) by adding a coefficient for the amplitude and the peak location, which is determined numerically. The analytical approximation for the position of the first acoustic peak used here is

$$\ell_p = 0.746\pi \sqrt{3(1+z_r)} \frac{R(\omega_m, \omega_k, y)}{I_s(\omega_m, \omega_b)}, \quad (14)$$

where  $\omega_\star \equiv \Omega_\star h^2$ , and  $R = \omega_m^{1/2} [\sinh(\omega_k^{1/2} y)] / \omega_k^{1/2}$ ,  $\omega_m^{1/2} y$ ,  $\omega_m^{1/2} [\sin(|\omega_k|^{1/2} y)] / |\omega_k|^{1/2}$  for open, flat and closed models

respectively. Here  $y(\omega_m, \omega_k, \omega_\Lambda)$  is given by formula (8b) and  $I_s(\omega_m, \omega_b)$  by formulae (17)–(19) of Efstathiou & Bond (1999). The accuracy of this analytical approximation is better than 1 per cent.

The approximation for the amplitude of the first acoustic peak is as follows:

$$A_p = \left[ \frac{\ell_p(\ell_p + 1)}{2\pi} C_2 \frac{\Gamma\left(\ell_p + \frac{n_s + 1}{2}\right)}{\Gamma\left(\ell_p + \frac{5 - n_s}{2}\right)} \times \frac{\Gamma\left(\frac{9 - n_s}{2}\right)}{\Gamma\left(\frac{3 + n_s}{2}\right)} + 0.838A(\omega_b, \omega_{\text{cdm}}, n_s) \right]^{1/2}, \quad (15)$$

where  $\ln A(\omega_b, \omega_{\text{cdm}}, n_s) = 4.5(n_s - 1) + a_1 + a_2\omega_{\text{cdm}}^2 + a_3\omega_{\text{cdm}} + a_4\omega_b^2 + a_5\omega_b + a_6\omega_b\omega_{\text{cdm}} + a_7\omega_k$ , with  $a_1 = 2.376$ ,  $a_2 = 3.681$ ,  $a_3 = -5.408$ ,  $a_4 = -54.262$ ,  $a_5 = 18.909$ ,  $a_6 = 15.384$ ,  $a_7 = 4.2$ , and  $C_2$  is the quadrupole anisotropy approximated by

$$C_2 = A_s \frac{\pi}{16} \left(\frac{H_0}{c}\right)^{n_s+3} \frac{\Gamma(3 - n_s)}{\Gamma^2\left(\frac{4 - n_s}{2}\right)} \frac{\Gamma\left(2 + \frac{n_s + 1}{2}\right)}{\Gamma\left(2 + \frac{5 - n_s}{2}\right)}. \quad (16)$$

The values  $a_1 - a_6$  are the best-fitting coefficients determined from a grid of models computed with CMBFAST (Efstathiou & Bond 1999). We have added the coefficient  $a_7$  in order to account for curvature. The accuracy of  $A_p$  in the parameter ranges that we consider is better than 5 per cent. We denote  $\ell_p$  and  $A_p$  by  $y_{14}$  and  $y_{15}$  respectively.

The theoretical values of the other experimental constraints are obtained as follows: the density fluctuation  $\sigma_8$  is calculated according to equation (1) with  $P(k; z)$  taken from equation (11). We set  $y_{16} = \sigma_8\Omega_m^{\alpha_1}$ ,  $y_{17} = \sigma_8\Omega_m^{\alpha_2}$  and  $y_{18} = \sigma_8\Omega_m^{\alpha_3}$  with corresponding values of  $\alpha_i$  ( $i = 1, 2, 3$ ) for vanishing and non-zero curvature (see previous section).

The rms peculiar velocity of galaxies in a sphere of radius  $R = 50 h^{-1}$  Mpc is given by

$$V_{50}^2 = \frac{1}{2\pi^2} \int_0^\infty k^2 P^{(v)}(k) e^{-k^2 R_f^2} W^2(50 \text{ Mpc } k/h) dk, \quad (17)$$

where  $P^{(v)}(k)$  is the power spectrum for the velocity field of the density-weighted matter (Eisenstein & Hu 1999),  $W(50 \text{ Mpc } k/h)$  is the top-hat window function. A previous smoothing of the raw data with a Gaussian filter of radius  $R_f = 12 h^{-1}$  Mpc is employed, similar to the procedure which has led to the observational value. For the scales of interest  $P^{(v)}(k) \approx (\Omega^{0.6} H_0)^2 P(k; 0)/k^2$ . We denote the rms peculiar velocity by  $y_{19}$ .

The value by Gnedin (1998) from the formation of Ly $\alpha$  clouds constrains the rms linear density perturbation at redshift  $z = 3$  and wavenumber  $k_F = 38\Omega_m^{1/2} h \text{ Mpc}^{-1}$ . In terms of the power spectrum,  $\sigma_F$  is given by

$$\sigma_F^2(z) = \frac{1}{2\pi^2} \int_0^\infty k^2 P(k; z) e^{(-k/k_F)^2} dk. \quad (18)$$

It will be denoted by  $y_{20}$ . The corresponding value of the constraint by Croft et al. (1998) is

$$\Delta_p^2(k_p, z) \equiv k_p^3 P(k_p, z)/2\pi^2 \quad (19)$$

at  $z = 2.5$  with  $k_p = 0.008H(z)/(1+z)(\text{km s}^{-1})^{-1}$ , which will be denoted by  $y_{21}$ ;  $H(z) = H_0[\Omega_m(1+z)^3 + \Omega_k(1+z)^2 + \Omega_\Lambda]^{1/2}$  is the Hubble parameter at redshift  $z$ . The slope of the power spectrum at this scale and redshift,

$$n_p(z) \equiv \frac{\Delta \log P(k, z)}{\Delta \log k}, \quad (20)$$

is denoted by  $y_{22}$ .

For all tests except Gnedin's Ly $\alpha$  clouds, we use the density-weighted transfer function  $T_{\text{cb}\nu}(k, z)$  from (Eisenstein & Hu 1999). For Gnedin's  $\sigma_F$  we use  $T_{\text{cb}}(k, z)$  according to the prescription of Gnedin (1998). It must be noted that even in the model with maximal  $\Omega_\nu$  ( $\sim 0.2$ ) the difference between  $T_{\text{cb}}(k, z)$  and  $T_{\text{cb}\nu}(k, z)$  is less than 12 per cent for  $k \leq k_p$ . Early reionization changes the evolution of the density perturbation in the baryon component somewhat on small scales. This effect is not taken into account by the analytical approximation used here (Eisenstein & Hu 1999). Therefore, we restrict ourselves to models without early reionization. We calculate the Ly $\alpha$  tests according to the prescription given in section 5.4 of (Eisenstein & Hu 1999).

Finally, the values of  $\Omega_b h^2$ ,  $h$  and  $\Omega_m - 0.75\Omega_\Lambda$  are denoted by  $y_{23}$ ,  $y_{24}$  and  $y_{25}$  respectively.

The squared differences between the theoretical and observational values divided by the observational error are given by  $\chi^2$ ,

$$\chi^2 = \sum_{j=1}^{23} \left( \frac{\tilde{y}_j - y_j}{\Delta \tilde{y}_j} \right)^2. \quad (21)$$

Here  $\tilde{y}_j$  and  $\Delta \tilde{y}_j$  are the experimental data and their dispersion, respectively. The set of parameters  $\Omega_m, \Omega_\Lambda, \Omega_\nu, N_\nu, \Omega_b, h, n_s$  and  $b_{\text{cl}}$  are then determined by minimizing  $\chi^2$  using the Levenberg–Marquardt method (Press et al. 1992). The derivatives of the predicted values with respect to the search parameters that are required by this method are obtained numerically using a relative step size of  $10^{-5}$  with respect to the given parameter.

In order to test our method for stability, we have constructed a mock sample of observational data. We start with a set of cosmological parameters and determine the ‘observational’ data for them that would be measured in the case of faultless measurements with  $1\sigma$  errors comparable to the observational errors. We then insert random sets of starting parameters into the search program and try to recover the model that corresponds to the mock data. The method is stable if we can recover our input cosmological model (for more details of this test procedure see Novosyadlyj et al. (2000a). The code finds all the previously known parameters with high accuracy. Even starting very far away from the true values, our method is revealed as very stable and finds the ‘true’ model whenever possible. This means that the code finds the global minimum of  $\chi^2$  independent of the initial values for the parameters. This also hints that our data set is sufficiently diverse to be free of degeneracies (which plague parameter searches working with CMB data only).

## 4 RESULTS AND DISCUSSION

### 4.1 Calculations

The determination of the parameters<sup>1</sup>  $\Omega_m, \Omega_\Lambda, \Omega_\nu, N_\nu, \Omega_b, h, n_s$  and  $b_{\text{cl}}$  by the Levenberg–Marquardt  $\chi^2$  minimization method (Press et al. 1992) can be realized in the following way: we vary

<sup>1</sup> We treat  $\Omega_\Lambda$  and  $\Omega_m$  as free parameters,  $\Omega_k = 1 - \Omega_\Lambda - \Omega_m$ .

**Table 1.** Cosmological parameters determined from the LSS data described in the text without and with the SNIa constraint. The errors indicated are the square roots of the diagonal elements of the covariance matrix.

| $N_\nu$                   | $\chi^2_{\min}$ | $\Omega_m$      | $\Omega_\Lambda$ | $\Omega_\nu$    | $\Omega_b$        | $n_s$           | $h$             |
|---------------------------|-----------------|-----------------|------------------|-----------------|-------------------|-----------------|-----------------|
| Without SNIa constraint   |                 |                 |                  |                 |                   |                 |                 |
| 1                         | 5.90            | $0.37 \pm 0.06$ | $0.69 \pm 0.07$  | $0.03 \pm 0.03$ | $0.037 \pm 0.009$ | $1.02 \pm 0.04$ | $0.71 \pm 0.09$ |
| 2                         | 6.02            | $0.42 \pm 0.08$ | $0.64 \pm 0.09$  | $0.04 \pm 0.04$ | $0.038 \pm 0.010$ | $1.03 \pm 0.04$ | $0.71 \pm 0.09$ |
| 3                         | 6.17            | $0.47 \pm 0.10$ | $0.59 \pm 0.08$  | $0.06 \pm 0.01$ | $0.038 \pm 0.010$ | $1.04 \pm 0.03$ | $0.70 \pm 0.09$ |
| Including SNIa constraint |                 |                 |                  |                 |                   |                 |                 |
| 0–3                       | 6.02            | $0.32 \pm 0.05$ | $0.75 \pm 0.06$  | $<10^{-4}$      | $0.038 \pm 0.010$ | $1.0 \pm 0.05$  | $0.70 \pm 0.09$ |

the set of parameters  $\Omega_m, \Omega_\Lambda, \Omega_\nu, \Omega_b, h, n_s$  and  $b_{c1}$  with fixed  $N_\nu$  and find the minimum of  $\chi^2$ . As  $N_\nu$  can be discrete, we repeat this procedure three times for  $N_\nu = 1, 2$ , and 3. The lowest of the three minima is the minimum of  $\chi^2$  for the complete set of free parameters. Hence, we have seven free parameters. The formal number of observational points is 25 but, as we have mentioned, the 13 power spectra points can be described by just three degrees of freedom, so that the maximal number of truly independent measurements is 15. Therefore, the number of degrees of freedom for our search procedure is  $N_F = N_{\text{exp}} - N_{\text{par}} = 8$  if all observational points are used. In order to investigate to what extent the LSS constraints on fundamental parameters match the constraints implied by SNIa (Perlmutter et al. 1999), we have determined all eight parameters with and without the SNIa constraint ( $\bar{y}_{25}$ ). The results are presented in Table 1.

Note, that for all models  $\chi^2_{\min}$  is in the range  $N_F - \sqrt{2N_F} \leq \chi^2_{\min} \leq N_F + \sqrt{2N_F}$  which is expected for a Gaussian distribution of  $N_F$  degrees of freedom. This means that the cosmological paradigm which has been assumed is in agreement with the data. (Note here that the reduction of the 13 independent data points of the cluster power spectrum to three parameters is not important for our analysis, because removing them from the search procedure does not change the results essentially, as we will see later.)

Let us investigate how the parameters of the best-fitting model vary if we also include the data of the MAXIMA-1 experiment. The location and amplitude of the first acoustic peak determined from the combined Boomerang and MAXIMA-1 data are (Hu et al. 2001)  $\ell_p = 206 \pm 6$ ,  $A_p = 78.6 \pm 7$ . If we use them instead of the values used above, the best-fitting parameters remain practically unchanged,  $\Omega_m = 0.37 \pm 0.06$ ,  $\Omega_\Lambda = 0.66 \pm 0.06$ ,  $\Omega_\nu = 0.03 \pm 0.03$ ,  $N_\nu = 1$ ,  $\Omega_b = 0.039 \pm 0.010$ ,  $n_s = 1.05 \pm 0.04$ , and  $h = 0.70 \pm 0.09$ . Hence, including the MAXIMA-1 data in the determination of the first acoustic peak is not essential in our analysis and we will use here the values determined from the Boomerang data alone. This is however an important confirmation of the consistency of the two data sets.

We have also analysed the influence of the amplitudes of the second and third acoustic peaks on the determination of cosmological parameters in the frame of our approach. If we add to our data set their values and errors as determined by (Hu et al. 2001) and calculate them using the analytical approximation given by the same authors then  $\chi^2 \approx 18$ , which is far too much for 9 degrees of freedom. In this case the best-fitting parameters are  $\Omega_m = 0.37 \pm 0.07$ ,  $\Omega_\Lambda = 0.72 \pm 0.05$ ,  $\Omega_\nu \approx 0$ ,  $\Omega_b = 0.046 \pm 0.011$ ,  $n_s = 0.97 \pm 0.03$  and  $h = 0.67 \pm 0.08$ . For the second acoustic peak and nucleosynthesis constraint the deviations of the

predicted values from their observed counterparts are maximal ( $2.8\sigma$  higher, and  $1.4\sigma$  higher respectively). If we exclude the nucleosynthesis constraint from the search procedure then  $\chi^2/N_F \approx 7/8$  and the best-fitting parameters become  $\Omega_m = 0.34 \pm 0.06$ ,  $\Omega_\Lambda = 0.74 \pm 0.05$ ,  $\Omega_\nu \approx 0$ ,  $\Omega_b = 0.055 \pm 0.012$ ,  $n_s = 0.98 \pm 0.03$  and  $h = 0.72 \pm 0.08$ . Practically all used constraints are satisfied but  $\Omega_b/h^2$  is  $9\sigma$  higher than value deduced from the determination of the primeval deuterium abundance by (Burles et al. 1999) and  $12\sigma$  higher than more recent value (Burles et al. 2001). This problem of the inconsistency of the Boomerang and MAXIMA-1 values for the height of the second peak, especially with the nucleosynthesis constraint on the baryon abundance, has been discussed at large in the recent literature (Tegmark & Zaldarriaga 2000b; Durrer, Kunz & Melchiorri 2001; Esposito et al. 2001; Hu et al. 2001; Lange et al. 2001). As we have nothing new to add to this subject here, we will not discuss it any further in this work. In what follows, we exclude the second and third acoustic peaks from experimental data set in our search procedure but we will use them in the discussion of our best-fitting model.

The errors in the best-fitting parameters as presented in Table 1 are the square roots of the diagonal elements of the covariance matrix which is calculated according to the prescription given in Press et al. 1992 (chapter 15) or Tegmark & Zaldarriaga 2000a (appendix A).

## 4.2 The best-fitting model

The model with one sort of massive neutrinos provides the best fit to the data,  $\chi^2_{\min} = 5.9$ . However, there is only a marginal difference in  $\chi^2_{\min}$  for  $N_\nu = 1, 2, 3$ . With the given accuracy of the data we cannot conclude whether massive neutrinos are present at all and if they are, what number of degrees of freedom is favoured. We summarize that the considered observational data on LSS of the Universe can be explained by a  $\Lambda$ CDM inflationary model with a scale-invariant spectrum of scalar perturbations and a small positive curvature.

Including the SNIa constraint in the experimental data set decreases  $\Omega_m$ , increases  $\Omega_\Lambda$  slightly and favours  $\Omega_\nu \approx 0$ , a  $\Lambda$ CDM model.

In Table 2 we compare the values of the different observational constraints with the predictions for the best-fitting models (Table 1 for  $N_\nu = 1$ ). In both cases the calculated characteristics of the LSS are within the  $1\sigma$  error bars of the observed values. In the last row we indicate the age of the Universe determined according to the general expression for non-zero curvature and non-zero  $\Lambda$  models

**Table 2.** Theoretical predictions for the used characteristics of the best-fitting  $\Lambda$ CDM model with one class of massive neutrinos with the cosmological parameters given in Table 1; first line (without SNIa constraint) and last line (including the SNIa constraint) are compared with observations.

| Characteristics                 | Observations <sup>a</sup>        | Predictions  |                |
|---------------------------------|----------------------------------|--------------|----------------|
|                                 |                                  | Without SNIa | Including SNIa |
| $\ell_p$                        | $197 \pm 6$                      | 197          | 197            |
| $A_p$                           | $69 \pm 8$                       | 71.5         | 71.9           |
| $V_{50}, \text{km s}^{-1}$      | $375 \pm 85$                     | 327          | 308            |
| $\sigma_8 \Omega_m^{0.21}$      | $0.60 \pm 0.022$                 | 0.61         | 0.60           |
| $\sigma_8 \Omega_m^{0.22}$      | $0.56 \pm 0.095$                 | 0.58         | 0.58           |
| $\sigma_8 \Omega_m^{0.23}$      | $0.8 \pm 0.1$                    | 0.69         | 0.71           |
| $\sigma_F$                      | $2.0 \pm .3$                     | 1.9          | 1.9            |
| $\Delta_\rho^2(k_p)$            | $0.57 \pm 0.26$                  | 0.56         | 0.59           |
| $n_p(k_p)$                      | $-2.25 \pm 0.2$                  | -2.20        | -2.20          |
| $h$                             | $0.65 \pm 0.10$                  | 0.71         | 0.70           |
| $\Omega_b h^2$                  | $0.019 \pm 0.0012$               | 0.019        | 0.019          |
| $\Omega_m - 0.75\Omega_\Lambda$ | $-0.25 \pm 0.125$                | -0.14        | -0.25          |
| $t_0, \text{Gyr}^b$             | $13.2 \pm 3.0^c, 11.5 \pm 1.5^d$ | 12.6         | 13.5           |

<sup>a</sup> All errors are  $\pm 1\sigma$ .

<sup>b</sup> Is not used in the search procedure.

<sup>c</sup> (Carretta et al. 2000).

<sup>d</sup> (Chaboyer et al. 1998).

(Sahni & Starobinsky 2000)

$$t_0 = H_0^{-1} \int_0^\infty \frac{dz}{\Omega_m(1+z)^5 + \Omega_k(1+z)^4 + \Omega_\Lambda(1+z)^2}. \quad (22)$$

The predicted age of the Universe agrees well with recent determinations of the age of globular clusters. Comparing the results obtained without and with the SNIa constraint, we conclude that the values of the fundamental cosmological parameters  $\Omega_m$ ,  $\Omega_\Lambda$  and  $\Omega_k$  determined by the observational characteristics of large-scale structure match the SNIa test very well. This can be interpreted as independent support of the SNIa result in the framework of the standard cosmological paradigm. However, in order to elucidate how LSS data constrain cosmological parameters, we analyse further only the model obtained without the SNIa constraint.

The best-fitting values of cosmological parameters determined by LSS characteristics<sup>2</sup> are  $\Omega_m = 0.37 \pm 0.06$ ,  $\Omega_\Lambda = 0.69 \pm 0.07$ ,  $\Omega_\nu = 0.03 \pm 0.03$ ,  $N_\nu = 1$ ,  $\Omega_b = 0.037 \pm 0.009$ ,  $n_s = 1.02 \pm 0.04$  and  $h = 0.71 \pm 0.09$ . The CDM density parameter is  $\Omega_{\text{cdm}} = 0.30 \pm 0.10$  and  $\Omega_k = -0.06 \pm 0.13$ . The neutrino content, which is compatible with zero, is very badly determined (100 per cent error). The obtained value should be interpreted as an upper limit to the neutrino contribution. Below we will discuss this upper limit in more detail.

The value of the Hubble constant is close to the result by Madore et al. (1999) and Mould et al. (2000), somewhat higher than the directly measured value given in equation (8). The spectral index coincides with the prediction of the simplest inflationary scenario: it is close to unity. The neutrino matter density  $\Omega_\nu = 0.03$  corresponds to a neutrino mass of  $m_\nu = 94\Omega_\nu h^2 \approx 1.4 \text{ eV}$  but is compatible with 0 within  $1\sigma$ . The estimated cluster bias parameter  $b_{\text{cl}} = 2.36 \pm 0.25$  fixes the amplitude of the Abell–ACO power spectrum (Fig. 1).

Recently, it has been shown (Novosyadlyj 1999) that, owing to the large error bars, the position of the peak of  $\tilde{P}(k)$  at

<sup>2</sup> We still include the direct measurement of  $h$  and the nucleosynthesis constraint in the analysis.

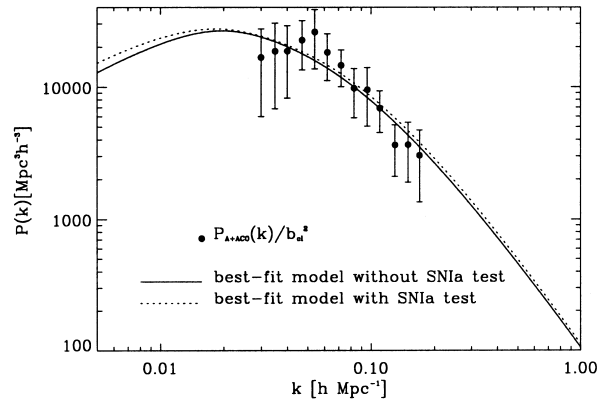


**Figure 1.** The observed Abell–ACO power spectrum (filled circles) and the theoretical spectra predicted by closed  $\Lambda$ CDM models with parameters taken from Table 1 ( $N_\nu = 1$ ).

$k \approx 0.05 h \text{ Mpc}^{-1}$  does not influence the determination of cosmological parameters significantly. Only the slope of the power spectrum on scales smaller than the scale of the peak is relevant for cosmological parameters. On the other hand, the relation of the peak in  $\tilde{P}_{\text{A+ACO}}(k)$  obtained from the space distribution of Abell–ACO clusters around us to the matter density of the power spectrum of the entire Universe is still under discussion. Using numerical simulations, Retzlaff et al. (1998) have shown that the pronounced peak in the spectrum (the fifth data point in Fig. 1) could be purely caused by cosmic variance. Therefore, it should not influence cosmological parameters. In fact, the maximum of our fitting curve is at a different position, which shows that this peak position is not relevant for the present work. The oscillation of the  $\tilde{P}_{\text{A+ACO}}(k)$  around the best-fitting  $P(k)$  in Fig. 1 determined from all observable data on LSS reflects the real distribution of rich clusters of galaxies in the vicinity of  $\sim 300 h^{-1} \text{ Mpc}$  of our own Galaxy only. This is supported by similar features in spectra reconstructed from the expanded sample of Abell–ACO clusters (Miller & Batuski 2000) and IRAS Point Source Catalog Redshift Survey (Hamilton, Tegmark & Padmanabhan 2000; Tegmark & Padmanabhan 2000; Saunders et al. 2000).

Using CMBFAST we have calculated the angular power spectra of CMB temperature fluctuations for both best-fitting models. Comparison with the COBE, Boomerang and MAXIMA-1 experiments is shown in Fig. 2. The CMB power spectrum predicted by both best-fitting models matches the data very well within the range of the first acoustic peak. However, it does not reproduce the absence of a second peak inferred from the Boomerang and MAXIMA-1 data at  $\ell > 350$ . This problem has been discussed intensively in literature (Tegmark & Zaldarriaga 2000b; Esposito et al. 2001; Hu et al. 2001; Lange et al. 2001). The lack of power in this range strongly favours models with more baryons than compatible with standard cosmological nucleosynthesis. The MAXIMA-1 data reduces the problem somewhat but does not remove it entirely (Hu et al. 2000). However, as we shall discuss, the cosmological parameters which match Boomerang and MAXIMA-1 data at high spherical harmonics also strongly disagree with other LSS constraints used here (see Subsection 4.8 below). Furthermore, the Boomerang, MAXIMA-1 and other CMB data in this range do not match each other very well. This (and the amount of work already published on this subject, some of which is cited above) prompted us to ignore the problem of the second peak in the CMB anisotropy spectrum in this work. Future flights of Boomerang and MAXIMA and/or the future projects

MAP and Planck will certainly decide on this very important issue, but we consider it premature to draw very strong conclusions at this point.

Finally let us mention some global characteristics of a Universe with our best-fitting cosmological parameters. Its age of  $t_0 = 12.6$  Gyr is in the range of values determined from the age of globular clusters (Chaboyer et al. 1998; Carretta et al. 2000). The deceleration parameter is  $q_0 = -0.52$ , in good agreement with the SNIa constraint presented above leading to (Perlmutter et al. 1998)  $\tilde{q}_0 = -0.57 \pm 0.17$ . The original deceleration ( $q > 0$ ) changes into acceleration ( $q < 0$ ) at the redshift  $z_d \approx 0.55$ . The ‘equality epoch’,  $\rho_m(z_e) = \rho_\Lambda(z_e)$ , corresponds to the redshift  $z_e \approx 0.23$ .

### 4.3 The influence of different experimental data

One important question is how sensitive our result responds to each data point. To estimate this, we exclude some data points from the search routine and redetermine the best-fitting parameters. The results of this procedure are presented in Table 3. In all cases when data on the first acoustic peak are included  $\Omega_m + \Omega_\Lambda \approx 1.06$ , there is very slight positive curvature ( $\Omega_k \approx -0.06$ ) but compatible with a flat universe, i.e. the geometry is defined mainly by the position of the first acoustic peak. The LSS data without CMB measurements favour an open Universe with  $\Omega_k = 0.14$  (fourth row in Table 3). The value of  $\Omega_m$  never exceeds 0.56,

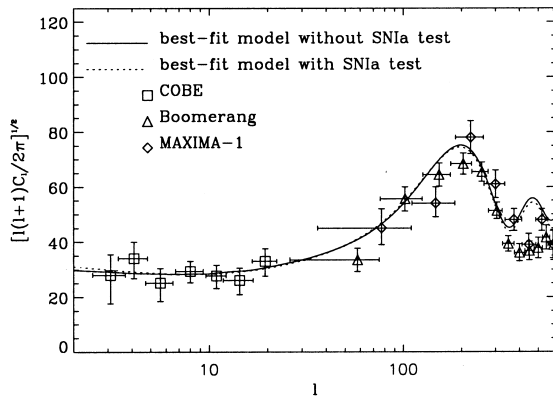


**Figure 2.** The CMB power spectra predicted by best-fitting  $\Lambda$ CDM models with parameters from Table 1 ( $N_\nu = 1$ ) and COBE DMR (Bennett et al. 1996), Boomerang (de Bernardis et al. 2000) and MAXIMA-1 (Hanany et al. 2000) experimental data.

$\Omega_\Lambda$  is always larger 0.47 and in most cases  $\Omega_\Lambda > \Omega_m$ . The best-fitting values of the spectral index  $n_s$  and  $h$  for the different observable data sets are in the relatively narrow ranges of 0.99–1.14 and 0.67–0.72 respectively. The baryon content,  $\Omega_b$ , is fixed by the nucleosynthesis constraint. Without this constraint (row 12 in Table 3)  $\Omega_b$  is lower,  $\Omega_b \approx 0.001$ , even below the value inferred from the luminous matter in the Universe,  $\Omega_{\text{lum}} \sim 7 \times 10^{-3}$ .

The hot dark matter content,  $\Omega_\nu$ , is reduced mainly by the Ly $\alpha$  constraints but it is poorly determined in all cases. If instead of or together with these Ly $\alpha$  constraints we use those by McDonald et al. (2000), which reduce the power at small scales, then the best-fitting value for the neutrino content is  $\approx 0.07$ . In this case, the predictions for Ly $\alpha$  constraints by Gnedin (1998) and Croft et al. (1998) are out of their  $1\sigma$  ranges. Moreover, the constraints by McDonald et al. (2000) are not in good agreement with other data, especially, Bahcall & Fan (1998) and the SNIa constraints. We have not included these constraints any further in our determination of cosmological parameters. Note however that the neutrino content is mainly constrained by the Ly $\alpha$  data. If both Ly $\alpha$  tests are excluded, the best-fitting value of  $\Omega_\nu$  rises to 0.21!

Excluding the direct measurement of the Hubble parameter from our search procedure leads to a substantially larger value of  $h \sim 0.91$  which is in disagreement with the direct determination.

The comparison of the first and second rows of Table 3 shows that the Abell–ACO power spectrum favours a slope of the matter power spectrum in the range  $0.02 \leq k \leq 0.1 h \text{ Mpc}^{-1}$ ,  $n \sim -1.5$ , which results in lowering  $\Omega_\Lambda$  and introduces a small but non-zero neutrino content.

The constraints  $\tilde{\sigma}_8 \Omega_m^{\alpha_2}$  (Viana & Liddle 1999) and  $\Delta_p^2(k_p)$  have almost no influence on the determination of parameters (rows 6, 10 and 15) owing to their large error bars. They can be removed from the data set, which reduces the number of effective degrees of freedom to  $N_F = 5$ ; this is important for the marginalization procedure.

### 4.4 Marginalization

The next important question is: ‘which is the confidence limit for each parameter marginalized over the others?’. The straight forward answer is the integral of the likelihood function over the allowed range of all the other parameters. But for a seven-dimensional parameter space this is computationally time-consuming. Therefore, we estimate the  $1\sigma$  confidence limits for

**Table 3.** Best-fitting values of cosmological parameters determined from the different data sets.

| No | Data set  | $\chi^2_{\text{min}}/N_F$ | $\Omega_m$ | $\Omega_\Lambda$ | $\Omega_\nu$ | $\Omega_b$ | $n_s$ | $h$  |
|----|---|---------------------------|------------|------------------|--------------|------------|-------|------|
| 1  | All observable data points are used   | 5.90/7                    | 0.37       | 0.69             | 0.027        | 0.037      | 1.02  | 0.71 |
| 2  | $\tilde{P}_{A+\text{ACO}}(k)$ 's points are excluded                                      | 2.12/4                    | 0.32       | 0.75             | 0.0          | 0.039      | 1.00  | 0.70 |
| 3  | $\tilde{\ell}_p, \tilde{A}_p$ are excluded  | 4.79/5                    | 0.39       | 0.47             | 0.058        | 0.042      | 1.14  | 0.67 |
| 4  | $\tilde{V}_{50}$ is excluded  | 5.54/6                    | 0.37       | 0.69             | 0.021        | 0.038      | 1.00  | 0.71 |
| 5  | $\tilde{\sigma}_8 \Omega_m^{\alpha_2}$ is excluded  | 4.58/6                    | 0.45       | 0.61             | 0.052        | 0.039      | 1.03  | 0.69 |
| 6  | $\tilde{\sigma}_8 \Omega_m^{\alpha_2}$ is excluded  | 5.88/6                    | 0.37       | 0.69             | 0.027        | 0.037      | 1.02  | 0.71 |
| 7  | $\tilde{\sigma}_8 \Omega_m^{\alpha_3}$ is excluded  | 4.72/6                    | 0.38       | 0.68             | 0.028        | 0.038      | 1.01  | 0.70 |
| 8  | All $\sigma_8$ tests are excluded   | 3.85/4                    | 0.49       | 0.57             | 0.060        | 0.041      | 1.04  | 0.68 |
| 9  | the first Ly $\alpha$ test is excluded  | 5.46/6                    | 0.42       | 0.65             | 0.048        | 0.039      | 1.02  | 0.70 |
| 10 | The second Ly $\alpha$ test is excluded   | 5.81/5                    | 0.37       | 0.69             | 0.026        | 0.037      | 1.02  | 0.71 |
| 11 | Both Ly $\alpha$ tests are excluded   | 4.49/4                    | 0.56       | 0.50             | 0.21         | 0.042      | 1.04  | 0.67 |
| 12 | The nucleosynthesis constraint is excluded  | 4.52/6                    | 0.29       | 0.89             | 0.023        | 0.001      | 1.04  | 0.67 |
| 12 | The direct constraint on $h$ is excluded  | 4.18/6                    | 0.29       | 0.71             | 0.038        | 0.023      | 1.05  | 0.91 |
| 13 | Both previous constraints are excluded  | 4.16/5                    | 0.29       | 0.71             | 0.041        | 0.013      | 1.07  | 0.87 |
| 14 | $\tilde{V}_{50}, \tilde{\sigma}_8 \Omega_m^{\alpha_2}$ and $\Delta_p^2(k_p)$ are excluded | 5.52/4                    | 0.37       | 0.69             | 0.021        | 0.038      | 1.01  | 0.70 |
| 15 | $\tilde{\sigma}_8 \Omega_m^{\alpha_2}$ and $\Delta_p^2(k_p)$ are excluded                 | 5.88/5                    | 0.37       | 0.68             | 0.028        | 0.037      | 1.02  | 0.71 |



all parameters in the following way. By varying all parameters we determine the six-dimensional  $\chi^2$  hypersurface that contains 68.3 per cent of the total probability distribution. We then project this hypersurface on to each axis in parameter space. Its shadow on the parameter axes gives us the  $1\sigma$  confidence limits for the cosmological parameter under consideration. The  $1\sigma$  confidence limits obtained in this way for  $\Lambda$ MDM models with one sort of massive neutrino are given in Table 4. Including  $\tilde{\sigma}_8\Omega_m^{\alpha_2}$  and  $\tilde{\Delta}_\rho^2(k_p)$  does not change the marginalized limits significantly.

It must be noted that even though the upper  $1\sigma$  edge for  $h$  is 0.93 when marginalized over all other parameters for the data used here, the resulting age of the Universe is still larger than the lowest value allowed for the age of the oldest globular clusters,  $t_0 \approx 10$  Gyr if  $\Omega_\Lambda > 0.72$ . In Fig. 3 we present the constraints in the  $\Omega_\Lambda - h$  plane given by the lower limit for the age of the Universe, 10 Gyr, for models with zero and positive curvature. The range above the corresponding line is excluded by this limit. Thus, the lower limit for the age of the Universe additionally constrains the confidence limits on the parameters,  $h$  and  $\Omega_k$  from above and  $\Omega_\Lambda$  from below.

We have repeated the marginalization procedure including the SNIa test (last column in Table 4). In this case we have to use all input data points (15 independent measurements), because neglecting  $\tilde{\sigma}_8\Omega_m^{\alpha_2}$  and  $\tilde{\Delta}_\rho^2(k_p)$  does somewhat change the marginalized limit. Hence, the number of degrees of freedom is  $N_F = 8$  ( $1\sigma$  confidence limits corresponding to  $\chi^2 \leq 15.3$ ). The SNIa test reduces the confidence ranges of  $\Omega_m$  and  $\Omega_\Lambda$  in spite of the larger number of degrees of freedom, but it results in somewhat wider

**Table 4.** The best-fitting values of all the parameters with errors obtained by maximizing the (Gaussian) 68 per cent confidence contours over all other parameters.

| Parameter        | Central value and errors  |                           |
|------------------|---------------------------|---------------------------|
|                  | without SNIa constraint   | with SNIa constraint      |
| $\Omega_m$       | $0.37^{+0.25}_{-0.15}$    | $0.32^{+0.20}_{-0.11}$    |
| $\Omega_\Lambda$ | $0.69^{+0.15}_{-0.20}$    | $0.75^{+0.10}_{-0.19}$    |
| $\Omega_\nu$     | $0.03^{+0.07}_{-0.03}$    | $0.0^{+0.09}_{-0.0}$      |
| $\Omega_b$       | $0.037^{+0.033}_{-0.018}$ | $0.038^{+0.033}_{-0.019}$ |
| $n_s$            | $1.02^{+0.09}_{-0.10}$    | $1.00^{+0.13}_{-0.10}$    |
| $h$              | $0.71^{+0.22}_{-0.19}$    | $0.70^{+0.28}_{-0.18}$    |
| $b_{cl}$         | $2.4^{+0.7}_{-0.6}$       | $2.2^{+0.8}_{-0.5}$       |

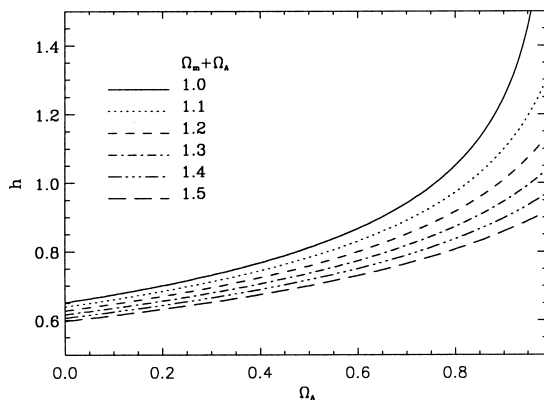


**Figure 3.** The lines in the  $\Omega_\Lambda - h$  plane corresponding to the lower limit on age of the Universe of 10 Gyr established from oldest globular cluster for models with zero and positive curvature. The range below the corresponding line is allowed.

$1\sigma$  error bars for the other parameters owing to the increase of  $N_F$  and the low accuracy of the added data points.

#### 4.5 The status of some subclasses of models

The errors presented in Table 4 define the range of each parameter within which, by adjusting the remaining parameters, a value of  $\chi^2_{\min} \leq 11.8$  can be achieved. Of course, the values of the remaining parameters always lie within their corresponding 68 per cent likelihoods given in Table 4. Models with vanishing  $\Lambda$  are outside this marginalized  $1\sigma$  range of the best-fitting model determined by the LSS observational characteristics used here, even without the SNIa constraint (column 2). Let us investigate the status of these models in more detail. For this, we set  $\Omega_\Lambda = 0$  as fixed parameter and determine the remaining parameters in the usual way. The minimal value of  $\chi^2$  is  $\chi^2 \approx 24$  with the following values for the other parameters:  $\Omega_m = 1.15$ ,  $\Omega_\nu = 0.22$ ,  $N_\nu = 3$ ,  $\Omega_b = 0.087$ ,  $n_s = 0.95$ ,  $h = 0.47$ ,  $b_{cl} = 3.7$  ( $\sigma_8 = 0.60$ ). This model is outside the  $2\sigma$  confidence contour of the best-fitting model for  $N_\nu = 3$  (Table 1 without SNIa test). The experimental data that disagree most with  $\Lambda = 0$  is that on the first acoustic peak. If we exclude it from the experimental data set,  $\chi^2_{\min} \approx 5.8$  for an open model with the following best-fitting parameters:  $\Omega_m = 0.48$ ,  $\Omega_\nu = 0.12$ ,  $N_\nu = 1$ ,  $\Omega_b = 0.047$ ,  $n_s = 1.3$ ,  $h = 0.64$ ,  $b_{cl} = 2.5$  ( $\sigma_8 = 0.82$ ). This model is inside the  $1\sigma$  confidence contour of the best-fitting  $\Lambda$ MDM model obtained without data on the first acoustic peak (row 3 of Table 3). The reason for this behaviour is clear: the position of the ‘kink’ in the matter power spectrum at large scales demands a ‘shape parameter’  $\Gamma = \Omega_m h^2 \sim 0.25$ , which can be achieved either by choosing an open model or allowing for a cosmological constant. The position of the acoustic peak that demands an approximately flat model then closes the first possibility.

Results change only slightly if instead of the Boomerang data we use Boomerang+MAXIMA-1 as discussed in Section 4.1. Hence, we can conclude that the LSS observational characteristics together with the Boomerang (+MAXIMA-1) data on the first acoustic peak already rule out zero- $\Lambda$  models at more than 95 per cent confidence level and actually demand a cosmological constant in the same bulk part as direct measurements. We consider this a non-trivial consistency check!

Flat  $\Lambda$  models, in contrast, are inside the  $1\sigma$  contour of our best-fitting model. Actually, the best-fitting flat model has  $\chi^2_{\min} \approx 8.3$  and the best-fitting parameters  $\Omega_m = 0.35 \pm 0.05$ ,  $\Omega_\Lambda = 0.65 \mp 0.05$ ,  $\Omega_\nu = 0.04 \pm 0.02$ ,  $N_\nu = 1$ ,  $\Omega_b = 0.029 \pm 0.005$ ,  $n_s = 1.04 \pm 0.06$ ,  $h = 0.81 \pm 0.06$ ,  $b_{cl} = 2.2 \pm 0.2$  ( $\sigma_8 = 0.96$ ) are close to our previous (Novosyadlyj et al. 2000a) results with a somewhat different observational data set.

It is obvious that flat zero- $\Lambda$  CDM and MDM models are ruled out by the present experimental data set at an even higher confidence limit than by data without the Boomerang and MAXIMA-1 measurements in (Novosyadlyj et al. 2000a).

#### 4.6 Upper limits for the neutrino mass

As the neutrino content is compatible with zero, we determine an upper limit for it. We first determine the marginalized  $1\sigma$ ,  $2\sigma$  and  $3\sigma$  upper limits for  $\Omega_\nu$  for different values of  $N_\nu$ . Using the best-fitting value for  $h$  at given  $\Omega_\nu$ , we can then determine the corresponding upper limit for the neutrino mass,  $m_\nu = 94\Omega_\nu h^2 / N_\nu$ . The results are presented in Table 5. For more

**Table 5.** The upper limits for the neutrino content and mass (in eV) at different confidence levels.

| $N_\nu$ | 1 $\sigma$ C. L. |         | 2 $\sigma$ C. L. |         | 3 $\sigma$ C. L. |         |
|---------|------------------|---------|------------------|---------|------------------|---------|
|         | $\Omega_\nu$     | $m_\nu$ | $\Omega_\nu$     | $m_\nu$ | $\Omega_\nu$     | $m_\nu$ |
| 1       | 0.10             | 3.65    | 0.13             | 3.96    | 0.18             | 4.04    |
| 2       | 0.15             | 2.79    | 0.21             | 3.06    | 0.29             | 3.35    |
| 3       | 0.20             | 2.40    | 0.27             | 2.67    | 0.35             | 2.78    |

species of massive neutrino the upper limit for  $\Omega_\nu$  is somewhat higher but  $m_\nu$  is still lower for each confidence level. The upper limit for  $\Omega_\nu$  raises with the confidence level as expected. But the upper limit for the mass grows only very little because of the reduction of the best-fitting value for  $h$ . The upper limit for the combination  $\Omega_\nu h^2/N_\nu^{0.64}$  is approximately constant for all number species and confidence levels. The observational data set used here establishes an upper limit for the massive neutrino content of the Universe, which can be expressed in the form  $\Omega_\nu h^2/N_\nu^{0.64} \leq 0.042$  at  $2\sigma$  confidence level. The corresponding upper limit on the neutrino mass  $m_\nu \leq 4$  eV is close to the value obtained by Croft, Hu & Dave (1999).

#### 4.7 Limiting the tensor mode

Up to this point we ignored uncertainties in the *COBE* normalization. The statistical uncertainty of the fit to the four-year *COBE* data,  $\delta_h$ , is 7 per cent ( $1\sigma$ ) (Bunn & White 1997) and we want to study how this uncertainty influences the accuracy of cosmological parameters that we determine.

Varying  $\delta_h$  in the  $1\sigma$  range, we found that the best-fitting values of all parameters except  $\Omega_\nu$ , do not vary by more than 7 per cent from the values presented in Table 1. Only  $\Omega_\nu$ , for which  $1\sigma$  errors are of the order of 100 per cent, varies in a range of 20 per cent. These uncertainties are significantly smaller than the standard errors given in Table 1 and ignoring them is thus justified. (Including this error raises our standard  $1\sigma$  errors from typically 10–20 per cent to 11–21 per cent.)

Our results depend on a possible tensor component only via the *COBE* data which enters our calculation through the normalization constant  $\delta_h$ , in equations (11) and (12). We can estimate the maximal contribution of a tensor mode in the *COBE*  $\Delta T/T$  data in the following way: we disregard the *COBE* normalization and consider  $\delta_h$  as free parameter to be determined like the others. Its best-fitting value then becomes  $\delta_h^{\text{LSS}} = (2.95 \pm 2.55) \times 10^{-5}$  (for  $N_\nu = 1$ ), while the best-fitting values of the other parameters are  $\Omega_m = 0.40 \pm 0.08$ ,  $\Omega_\Lambda = 0.66 \pm 0.07$ ,  $\Omega_\nu = 0.05 \pm 0.05$ ,  $\Omega_b = 0.038 \pm 0.010$ ,  $n_s = 1.14 \pm 0.31$ ,  $h = 0.71 \pm 0.09$  and  $b_{\text{cl}} = 2.4 \pm 0.3$ . The best-fitting value for density perturbation at horizon scale from the 4-year *COBE* data for this set of parameters is larger than the best-fitting value determined from LSS characteristics,  $\delta_h^{\text{COBE}} = 4.0 \times 10^{-5} > \delta_h^{\text{LSS}}$ . This means that *COBE*  $\Delta T/T$  data may contain a non-negligible tensor contribution. The most likely value of its fraction is given by  $T/S = (\delta_h^{\text{COBE}} - \delta_h^{\text{LSS}})/\delta_h^{\text{LSS}}$ . This value is  $T/S = 0.36$  for the corresponding best-fitting values of  $\delta_h^{\text{COBE}}$  and  $\delta_h^{\text{LSS}}$  from the Boomerang data alone and  $T/S = 0.18$  from the combined Boomerang + MAXIMA-1 data. As the standard error is rather large,  $\approx 90$  per cent, we determine upper confidence limits for  $T/S$  by marginalizing  $\delta_h^{\text{LSS}}$  over all the other parameters like we did for the neutrino content (see subsection 4.6). We then obtain  $T/S < 1$  at  $1\sigma$  confidence level and  $T/S < 1.5$  at  $2\sigma$  confidence level from

the Boomerang data alone for the amplitude and position of the first acoustic peak. If we use the combined Boomerang + MAXIMA-1 data these limits are somewhat lower, 0.9 and 1.3 correspondingly, because of the higher amplitude of the first acoustic peak measured by MAXIMA-1. The  $1\sigma$  upper constraint on the tensor mode obtained recently by Kinney, Melchiorri & Riotto (2001) from the Boomerang and MAXIMA-1 data on the CMB power spectrum for the same class of models ( $T/S < 0.8$  in our definition) is very close to the value obtained here.

#### 4.8 Comparison with other parameter estimations

The cosmological parameters determined here from LSS+CMB data agree well with the values obtained by other methods (see e.g. the review by Primack 2000). The marginalized  $1\sigma$  ranges are still rather large owing to the large experimental errors, the large number of parameters and the high degree of freedom. This, of course, does not mean that an arbitrary set of parameters within the marginalized ranges matches the experimental data set with an accuracy  $\leq 1\sigma$ .

We compare our best-fitting model with others found in the recent literature by testing our data set as well as the Boomerang and MAXIMA-1 data on the CMB power spectrum. At first we calculate the predictions of the following models for our data set:  $(\Omega_m, \Omega_\Lambda, \Omega_b, n_s, h) = \mathbf{P} = (0.49, 0.56, 0.054, 0.92, 0.65)$  obtained by Lange et al. (2001) as best-fitting model to the Boomerang and LSS data (denoted there as model P9);  $\mathbf{P} = (0.68, 0.23, 0.07, 1.0, 0.6)$  obtained by Balbi et al. (2000) as best-fitting model to the MAXIMA-1 and *COBE* DMR data;  $\mathbf{P} = (0.35, 0.65, 0.036, 0.95, 0.8)$  obtained by Hu et al. (2001) as best-fitting model to the Boomerang + MAXIMA-1 data on the first, second and third acoustic peaks;  $\mathbf{P} = (0.3, 0.7, 0.045, 0.975, 0.82)$  obtained by Jaffe et al. (2001) as best-fitting model to the Boomerang + MAXIMA-1 + *COBE* data on the CMB power spectrum; the ‘concordance’ model by Tegmark et al. (2000), which favours  $\mathbf{P} = (0.38, 0.62, 0.043, 0.91, 0.63)$ . Some authors give several sets of parameters obtained for different priors or by including different data sets; we take the one from which we obtain a minimal  $\chi^2$  for our data set. All these models have no massive neutrino component, no tensor mode and reionization is either not included or can be neglected. The predictions of cosmologies with the above parameters for the data considered in this work are presented in Table 6. The  $\chi^2$  presented in the last row includes also

$$\chi_{\text{A+ACO}}^2 = \sum_{i=1}^{13} \left[ \frac{P_{\text{A+ACO}}(k_i) - b_{\text{cl}}^2 P(k_i)}{\Delta P_{\text{A+ACO}}(k_i)} \right]^2,$$

which is small because of the cluster bias,  $b_{\text{cl}}$ , which is considered as a free parameter in each model. In spite of the fact that all parameters of each model are within the marginalized  $1\sigma$  ranges of the parameters of our best-fitting model, the total value of  $\chi^2$  for the entire parameter sets rules out all the models at more than  $2\sigma$  confidence level. Table 6 indicates the crucial tests. Models A and C are ruled out mainly by the nucleosynthesis constraint and the first  $\sigma_8$  test (cluster mass function). Model B strongly disagrees with all  $\sigma_8$  tests ( $14\sigma$ ,  $2.6\sigma$  and  $1.6\sigma$  correspondingly), both  $\text{Ly}\alpha$  tests ( $2.6\sigma$  and  $2.5\sigma$ ), the nucleosynthesis constraint ( $5.2\sigma$ ) and the data on the location of the first acoustic peak ( $5.6\sigma$ ). Moreover, models A and B do not match the SNIa test, which we have not included in  $\chi^2$ . Model D strongly disagrees with nucleosynthesis constraint ( $9.4\sigma$ ) and the Boomerang data on

**Table 6.** Theoretical predictions for the observational values by best-fitting models from the literature: A (Lange et al. 2001), B (Balbi et al. 2000), C (Hu et al. 2001), D (Jaffe et al. 2001), E (Tegmark et al. 2000).

| Characteristics                  | Observations       | Predictions |       |       |       |       |
|----------------------------------|--------------------|-------------|-------|-------|-------|-------|
|                                  |                    | A           | B     | C     | D     | E     |
| $\ell_p$                         | $197 \pm 6$        | 206         | 231   | 206   | 213   | 225   |
| $A_p$                            | $69 \pm 8$         | 57          | 68    | 63    | 72    | 62    |
| $V_{50}$ , km/s                  | $375 \pm 85$       | 280         | 310   | 303   | 293   | 239   |
| $\sigma_8 \Omega_m^{\alpha_1}$   | $0.60 \pm 0.022$   | 0.64        | 0.91  | 0.68  | 0.58  | 0.43  |
| $\sigma_8 \Omega_m^{\alpha_2}$   | $0.56 \pm 0.095$   | 0.62        | 0.93  | 0.65  | 0.65  | 0.42  |
| $\sigma_8 \Omega_m^{\alpha_3}$   | $0.8 \pm 0.1$      | 0.70        | 0.96  | 0.79  | 0.73  | 0.49  |
| $\sigma_F$                       | $2.0 \pm .3$       | 1.7         | 2.8   | 2.2   | 1.9   | 1.1   |
| $\Delta_\rho^2(k_p)$             | $0.57 \pm 0.26$    | 0.51        | 1.21  | 0.81  | 0.62  | 0.25  |
| $n_p(k_p)$                       | $-2.25 \pm 0.2$    | -2.25       | -2.15 | -2.21 | -2.22 | -2.30 |
| $h$                              | $0.65 \pm 0.10$    | 0.65        | 0.60  | 0.80  | 0.82  | 0.63  |
| $\Omega_b h^2$                   | $0.019 \pm 0.0012$ | 0.023       | 0.025 | 0.023 | 0.030 | 0.02  |
| $\Omega_m - 0.75 \Omega_\Lambda$ | $-0.25 \pm 0.125$  | 0.07        | 0.51  | -0.13 | -0.23 | -0.09 |
| $\chi^2$                         |                    | 27          | 285   | 39    | 105   | 106   |

**Table 7.** The  $\chi^2$  deviation of theoretical predictions for the CMB power spectrum from experimental results for the models in Table 6 and for our best-fitting model. The first number represents the value of  $\chi^2$  for the CMB power spectrum in the range of the first acoustic peak,  $50 \leq \ell \leq 375$ , the second number is for the entire range  $50 \leq \ell \leq 750$ . Clearly our model parameters are in serious disagreement with the experimental CMB data beyond the first acoustic peak.

| Experiment | $\chi^2$  |           |           |           |           | our best-fitting model |
|------------|-----------|-----------|-----------|-----------|-----------|------------------------|
|            | A         | B         | C         | D         | E         |                        |
| Boomerang  | 7.3/12.6  | 77.2/96.7 | 6.1/12.8  | 18.3/24.5 | 13.6/24.5 | 11.3/108.5             |
| MAXIMA-1   | 16.9/18.7 | 4.6/11.4  | 15.2/17.0 | 10.3/11.7 | 16.2/21.6 | 11.1/48.5              |

the location of the first acoustic peak ( $2.6\sigma$ ). Model E does not match first and third  $\sigma_8$  tests (at  $5.1\sigma$  and  $2.4\sigma$  respectively), the first Ly $\alpha$  test (at  $2.4\sigma$ ) and the data on the location of the first acoustic peak ( $3.2\sigma$ ). The latter is a result of the fact that the MAXIMA-1 peak position is more than  $1\sigma$  away from the peak position derived by the Boomerang data alone.

We now calculate the CMB power spectra for these models using CMBFAST (version 3.2) and compare them with the experimental data from Boomerang (de Bernardis et al. 2000) and MAXIMA-1 (Hanany et al. 2000). The  $\chi^2$  deviations for all models including our best-fitting model are presented in Table 7. The first number indicates the  $\chi^2$  for the range of the first acoustic peak,  $50 \leq \ell \leq 375$  (seven and five data points for the Boomerang and MAXIMA-1 experiments respectively), for the second number we have used the entire range,  $50 \leq \ell \leq 750$  (12 and 10 data points for the Boomerang and MAXIMA-1 experiments respectively). In the range of the first acoustic peak our model fits as well as the other models, but the observed power spectrum at higher spherical harmonics is not reproduced by our model, as we mentioned above.

Therefore, models which match the Boomerang and/or MAXIMA-1 CMB power spectrum at high spherical harmonics (in the range of the second and third acoustic peak) disagree with some of the  $\sigma_8$ , Ly $\alpha$  and/or nucleosynthesis constraints. Correspondingly, models which match very well the LSS observational characteristics predict a CMB power spectrum that disagrees with measurements by Boomerang and MAXIMA-1 on very small scales. The resolution of this problem can go in several directions. If the Boomerang and MAXIMA-1 measurements are confirmed, nucleosynthesis may have been more complicated than assumed for the constraint used in this work (Esposito et al. 2001). Another problem may be the cluster mass function constraint,

which is exponentially sensitive to the value of  $\sigma_8$  and might be too constraining, especially in view of all the uncertainties in the theory of cluster formation. Therefore, our constraint  $\sigma_8 \Omega_m^{\alpha_1} = 0.60 \pm 0.022$  has to be taken with a grain of salt and its incompatibility with, for example, the CMB data may also hint to a problem in the theory of cluster formation. Last but not least, if inconsistencies in the determination of cosmological parameters persist even after a serious improvement of data, e.g. with the Sloan Digital Sky Survey, this may hint that the correct model is not within the class considered. If we want to fit a snail within the class of all known mammals by  $\chi^2$  minimization (or by a much more sophisticated method), we never obtain a very convincing fit.

## 5 CONCLUSIONS

The main observational characteristics on LSS together with recent data on the amplitude and location of the first acoustic peak in the CMB power spectrum and the amplitude of the primordial power spectrum inferred by the COBE DMR 4-yr data, prefer a  $\Lambda$ MDM model with the following parameters:  $\Omega_m = 0.37^{+0.25}_{-0.15}$ ,  $\Omega_\Lambda = 0.69^{+0.15}_{-0.20}$ ,  $\Omega_\nu = 0.03^{+0.07}_{-0.03}$ ,  $N_\nu = 1$ ,  $\Omega_b = 0.037^{+0.033}_{-0.018}$ ,  $n_s = 1.02^{+0.09}_{-0.10}$ ,  $h = 0.71^{+0.22}_{-0.19}$ ,  $b_{cl} = 2.4^{+0.7}_{-0.7}$  ( $1\sigma$  marginalized ranges).

The central values correspond to a slightly closed ( $\Omega_k = -0.06$ )  $\Lambda$ MDM model with one class of 1.4-eV neutrinos. These neutrinos make up about 8 per cent of the clustered matter, baryons are 10 per cent and the rest (82 per cent) is in the form of a cold dark matter component. The energy density of clustered matter corresponds to only 35 per cent of the total energy density of matter plus vacuum, which amounts to  $\Omega = 1.06$ . The massive neutrino content is compatible with zero and we have established an upper limit in the form of  $\Omega_\nu h^2 / N_\nu^{0.64} \leq 0.042$  at  $2\sigma$

confidence level. The upper  $2\sigma$  limit for the neutrino mass is  $4.0\text{eV}$ .

If *COBE* normalization is disregarded, the best-fitting value of the density perturbation at horizon scale is  $\delta_h^{\text{LSS}} = (2.95 \pm 2.55) \times 10^{-5}$  while the best-fitting values of the other parameters are  $\Omega_m = 0.40$ ,  $\Omega_\Lambda = 0.66$ ,  $\Omega_\nu = 0.05$ ,  $N_\nu = 1$ ,  $\Omega_b = 0.038$ ,  $n_s = 1.14$ ,  $h = 0.71$  and  $b_{\text{cl}} = 2.4$ . Comparison of the best-fitting value with the *COBE* 4-yr data  $\delta_h^{\text{COBE}}$  gives an estimate for the contribution of a tensor mode to the *COBE* DMR data:  $T/S = 0.36_{-0.36}^{+0.64}$  from the Boomerang data on the first acoustic peak and  $T/S = 0.18_{-0.18}^{+0.72}$  ( $1\sigma$  confidence limits) when the combined Boomerang+MAXIMA-1 data are used. The upper limits on  $T/S$  at  $2\sigma$  confidence level for these two cases are 1.5 and 1.3 respectively.

The values for the matter density  $\Omega_m$  and the cosmological constant  $\Omega_\Lambda$  for the best-fitting model are close to those deduced from the SNIa test. Including this test in the observational data set results in a somewhat larger value of  $\Omega_\Lambda$  (7 per cent) and slightly lowers  $\Omega_m$ .

The observational characteristics of large-scale structure together with the Boomerang (+MAXIMA-1) data on the first acoustic peak rule out zero- $\Lambda$  models at more than  $2\sigma$  confidence limit.

## ACKNOWLEDGMENTS

It is a pleasure to acknowledge stimulating discussions with Stepan Apuneych, Pedro Ferreira, Vladimir Lukash, Max Tegmark and Matts Roos. This work is part of a project supported by the Swiss National Science Foundation (grant NSF 7IP050163). BN is also grateful to Geneva University for hospitality.

## REFERENCES

- Bahcall N. A., Fan X., 1998, *ApJ*, 504, 1  
 Balbi A. et al., 2000, *ApJ*, 545, L1  
 Bennett C. L. et al., 1996, *ApJ*, 464, L1  
 Benson A. J., Bower R. G., Frenk C. S., White S. D. M., 2000, *MNRAS*, 314, 517  
 Bertschinger E., Dekel A., Faber S. M., Dressler A., Burstein D., 1990, *ApJ*, 364, 370  
 Borgani S., Girardi M., Carlberg R. G., Yee H. K. C., Ellingson E., 1999, *ApJ*, 527, 561  
 Bridle S. L., Eke V. R., Lahav O., Lasenby A. N., Hobson M. P., Cole S., Frenk C. S., Henry J. P., 1999, *MNRAS*, 310, 565  
 Bunn E. F., White M., 1997, *ApJ*, 480, 6  
 Burles S., Nollett K. M., Truran J. N., Turner M. S., 1999, *Phys. Rev. Lett.*, 82, 4176  
 Burles S., Nollett K. M., Turner M. S., 2001, *ApJ*, 552, L1  
 Carroll S. M., Press W. H., Turner E. L., 1992, *ARA&A*, 30, 499  
 Carretta E., Gratton R. C., Clementini G., Fusi Pecci F., 1999, *ApJ*, 533, 215  
 Chaboyer B., Demarque P., Kernan P. J., Krauss L. M., 1998, *ApJ*, 494, 96  
 Courteau S., Faber S. M., Dressler A., Willick J. A., 1993, *ApJ*, 412, L51  
 Croft R. A. C., Weinberg D. H., Katz N., Hernquist L., 1998, *ApJ*, 495, 44  
 Croft R. A. C., Hu W., Dave R., 1999, *Phys. Rev. Lett.*, 83, 1092  
 Da Costa L. N., Vogeley M. S., Geller M. J., Huchra J. P., Park C., 1994, *ApJ*, 437, L1  
 de Bernardis P. et al., 2000, *Nat*, 404, 955  
 Dekel A., 1994, *ARA&A*, 32, 371  
 Dekel A., 2000, in Courteau S., Willick J., eds, *ASP Conf. Ser. Vol. 201, Cosmic Flows Workshop. Astron. Soc. Pac., San Francisco*, p. 240  
 Durrer R., Straumann N., 1999, New methods for the determination of cosmological parameters. Troisième Cycle de la Physique en Suisse Romande, Université de Lausanne  
 Durrer R., Kunz M., Melchiorri A., 2001, *Phys. Rev. D*, 63, 081301 (R)  
 Efstathiou G., Bond J. R., 1999, *MNRAS*, 304, 75  
 Einasto J. et al., 1997, *Nat*, 385, 139  
 Eisenstein D. J., Hu W., 1999, *ApJ*, 511, 5  
 Esposito S., Mangano G., Melchiorri A., Miele G., Pisanti O., 2001, *Phys. Rev. D*, 63, 043004  
 Fry J., Gaztañaga E., 1993, *ApJ*, 413, 447  
 Fukuda Y. et al., 1998, *Phys. Rev. Lett.*, 81, 1562  
 Girardi M. et al., 1998, *ApJ*, 506, 45  
 Gnedin N. Y., 1998, *MNRAS*, 299, 392  
 Hamilton A. J. S., Tegmark M., Padmanabhan N., 2000, *MNRAS*, 317, L23  
 Hanany S. et al., 2000, *ApJ*, 545, L5  
 Hu W., Fukugita M., Zaldarriaga M., Tegmark M., 2001, *ApJ*, 549, 669  
 Jaffe A. H. et al., 2001, *Phys. Rev. Lett.*, 86, 3475  
 Kinney W. H., Melchiorri A., Riotto A., 2001, *Phys. Rev. D*, 63, 023505  
 Kolatt T., Dekel A., 1997, *ApJ*, 479, 592  
 Landy S. D. et al., 1996, *ApJ*, 456, L1  
 Lange A. E. et al., 2001, *Phys. Rev. D*, 63, 042001  
 Liddle A. R., Lyth D. H., Viana P. T. P., White M., 1996, *MNRAS*, 282, 281  
 Lineweaver C. A., 1998, *ApJ*, 505, L69  
 Lineweaver C. A., Barbosa D., 1998, *ApJ*, 496, 624  
 Lyth D. H., Covi L., 2000, *Phys. Rev. D*, 62, 103504  
 McDonald P., Miralda-Escud J., Rauch M., Sargent W. L. W., Barlow T. A., Cen R., Ostriker J. P., 2000, *ApJ*, 543, 1  
 Maddox S. J., Efstathiou G., Sutherland W. J., 1996, *MNRAS*, 283, 1227  
 Madore B. F. et al., 1999, *ApJ*, 515, 2941  
 Melchiorri A. et al., 2000, *ApJ*, 536, L63  
 Miller C. J., Batuski D. J., 2001, *ApJ*, 551, 635  
 Mould J. R. et al., 2000, *ApJ*, 529, 786  
 Novosyadlyj B., 1999, *J. Phys. Stud.*, 3, 122  
 Novosyadlyj B., Durrer R., Gottlöber S., Lukash V. N., Apuneych S., 2000a, *A&A*, 356, 418  
 Novosyadlyj B., Durrer R., Gottlöber S., Lukash V. N., Apuneych S., 2000b, *Gravitation and Cosmology (suppl.)*, 6, 107  
 Park C., Vogeley M. C., Geller M. J., Huchra J. P., 1994, *ApJ*, 431, 569  
 Perlmutter S. et al., 1998, *Nat*, 391, 51  
 Perlmutter S. et al., 1999, *ApJ*, 517, 565  
 Press W. H., Flannery B. P., Teukolsky S. A., Vetterling W. T., 1992, *Numerical recipes in FORTRAN. Cambridge Univ. Press, New York*  
 Primack J. R., 2000, preprint (astro-ph/0007187)  
 Primack J. R., Gross M. A. K., 2000, preprint (astro-ph/0007165)  
 Retzlaff J., Borgani S., Gottlöber S., Klypin A., Muller V., 1998, *New Astron.*, 3, 631  
 Ricotti M., Gnedin N. Y., Shull J. M., 2000, *ApJ*, 534, 41  
 Riess A. et al., 1998, *AJ*, 116, 1009  
 Sahni V., Starobinsky A., 2000, *Int. J. Mod. Phys.*, D9, 373  
 Saunders W., Rowan-Robinson M., Lawrence A., 1992, *MNRAS*, 258, 134  
 Saunders W. et al., 2000, *MNRAS*, 317, 55  
 Seljak U., Zaldarriaga M., 1996, *ApJ*, 469, 437  
 Tadros H., Estathiou G., 1996, *MNRAS*, 282, 1381  
 Tadros H., Estathiou G., Dalton G., 1998, *MNRAS*, 296, 995  
 Tammann G. A., Federspiel M., 1997, in Livio M., Donahue M., Panagia N., eds, *The Extragalactic Distance Scale. Cambridge Univ. Press, Cambridge*, p. 137  
 Tegmark M., 1999, *ApJ*, 514, L69  
 Tegmark M., Zaldarriaga M., 2000a, *ApJ*, 544, 30

Tegmark M., Zaldarriaga M., 2000b, Phys. Rev. Lett., 85, 2240

Tegmark M., Zaldarriaga M., Hamilton A. J. S., 2001, Phys. Rev. D, 63,  
043007

Viana P. T. P., Liddle A. W., 1999, MNRAS, 303, 535

Vogeley M., Park C., Geller M. J., Huchra J. P., 1992, ApJ, 391, L5

This paper has been typeset from a  $\text{\TeX/L\AA\TeX}$  file prepared by the author.